

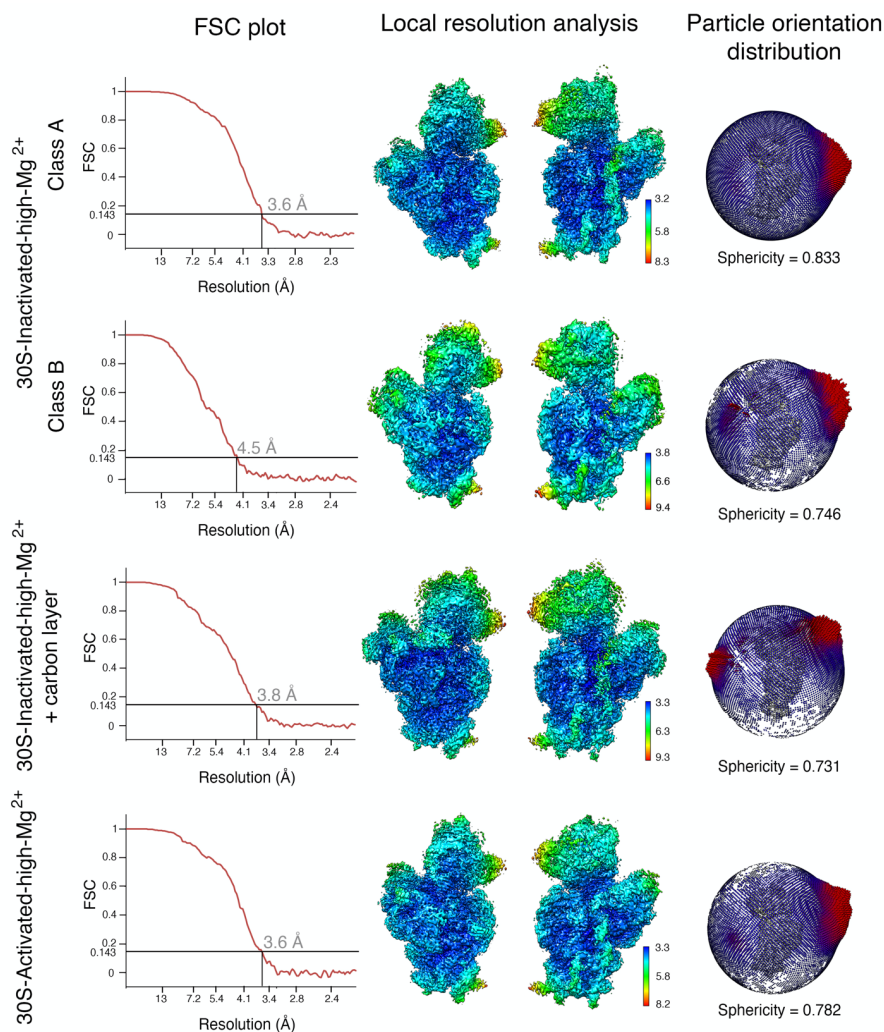
**Alternative Conformations and Motions Adopted by 30S  
Ribosomal Subunits Visualized by Cryo-Electron Microscopy**

Dushyant Jahagirdar, Vikash Jha, Kaustuv Basu, Josue Gomez-Blanco, Javier Vargas  
and Joaquin Ortega\*

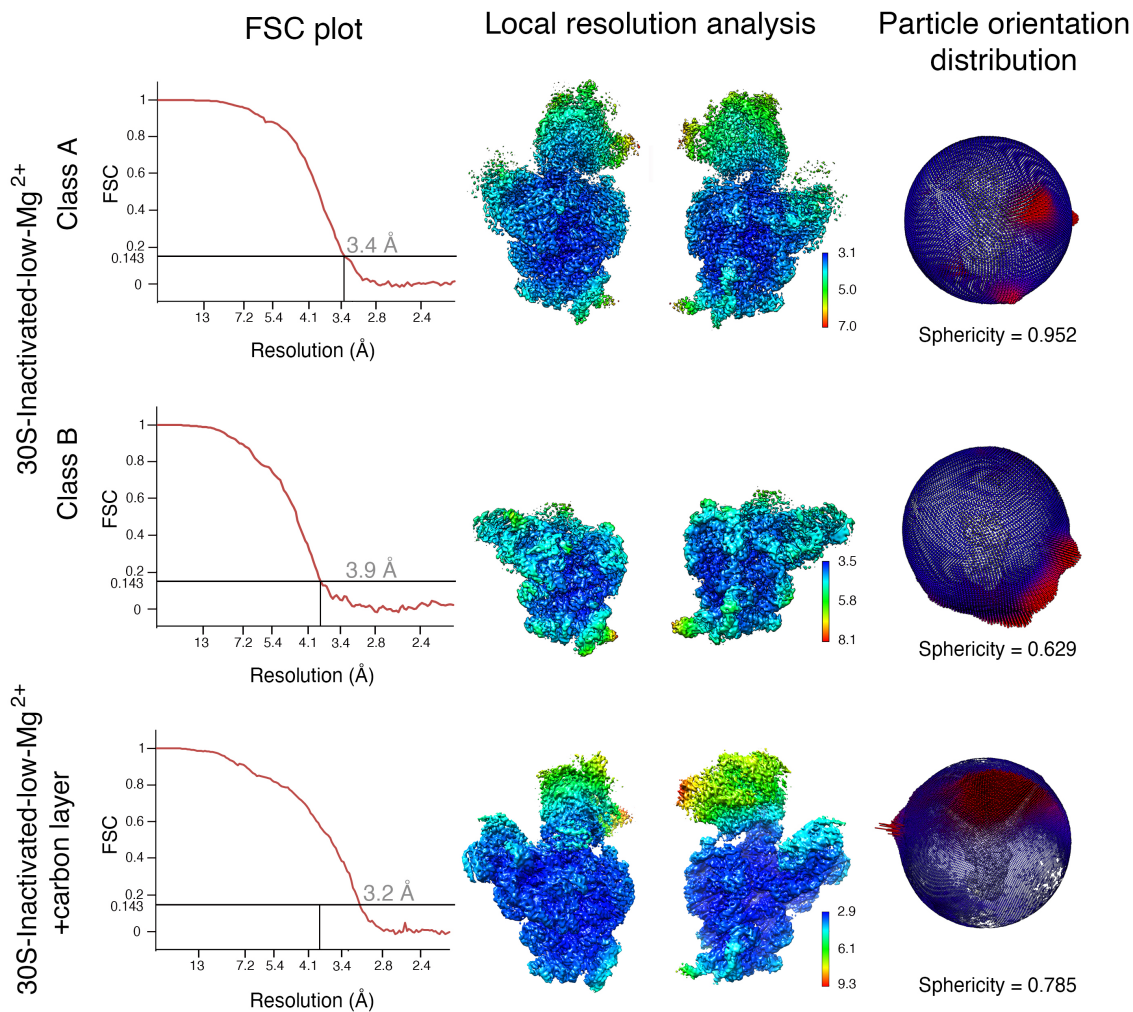
Department of Anatomy and Cell Biology, McGill University  
Montreal, Quebec H3A 0C7, Canada.

**This supplement contains:**  
Supplemental Figure S1-S2  
Supplemental Movies Captions  
Supplemental Table S1

## SUPPLEMENTAL FIGURE



**Supplemental Figure S1. Resolution analysis of the cryo-EM maps obtained under high Mg<sup>2+</sup> concentrations.** The left column shows the Fourier shell correlation (FSC) plots for the different cryo-EM maps obtained from samples maintained in buffer containing 10 mM magnesium acetate. Resolution is reported using FSC threshold of 0.143. The middle column displays the cryo-EM maps colored according to the local resolution analysis performed with RELION. The right column shows a sphere representing the angular distribution of the particles in each dataset. Each view angle is represented as a dot in the sphere. The height and color of the sphere relate to the number of particles representing each view. The areas in red indicate a higher number of particles representing those particular views.



**Supplemental Figure S2. Resolution analysis of the cryo-EM maps obtained under low Mg<sup>2+</sup> concentrations.** Fourier shell correlation (FSC) plots, local resolution analysis and angular distribution for the cryo-EM maps obtained from samples maintained in buffer containing 1.1 mM magnesium acetate. The layout of the figure is as in Supplemental Figure S1.

## SUPPLEMENTAL MOVIE CAPTIONS

**Supplemental Movie 1. Conformational transition between the canonical structure of the 30S subunit obtained by X-ray crystallography and the 30S-Inactivated-high-Mg<sup>2+</sup> particle.** The transition between conformations involves repositioning nucleotides 1532-1534 that are not forming any base pairing in the conventional structure to base pair with nucleotides 921-923. In this process, the bottom of helix 28 (region formed by nucleotides 1391-1396 and 921-925) and top of helix 44 formed in the canonical structure by nucleotides 1397-1407 and 1494-1503 become unfolded. The 3' end of the 16S rRNA (distal to nucleotide 1534) adopts a conformation similar to that adopted by mRNA during translation. The rRNA is displayed in light grey, the r-proteins in red. Helices 28, 44 and 45 are colored in navy blue except for the region on these helices that unfolds during the conformational change colored in yellow. Nucleotides 1532-1534 that upon the conformational transition form base pairs with nucleotides 921-923 are shown in red.

**Supplemental Movie 2-6. Main motions of the 30S particles.** Each movie shows the main motion represented by the first eigen vector in each type of 30S particle.

## SUPPLEMENTAL TABLE

**Supplemental Table S1.** Cryo-EM data acquisition, processing and map and model statistics.

	30S-Inactive high-Mg <sup>2+</sup> Class A	30S-Inactive high-Mg <sup>2+</sup> Class B	30S-Inactive high-Mg <sup>2+</sup> +carbon	30S-Activated high-Mg <sup>2+</sup>	30S-Inactive low-Mg <sup>2+</sup> Class A	30S-Inactive- low-Mg <sup>2+</sup> Class B	30S-Inactive- low-Mg <sup>2+</sup> +carbon	
<b>Data collection</b>								
Microscope	Titan Krios		Titan Krios	Titan Krios	Titan Krios		Titan Krios	
Detector	Falcon II		Falcon II	Falcon II	Falcon II		K3	
Nominal Magnification	75,000x		75,000x	75,000x	75,000x		81,000x	
Voltage (kV)	300		300	300	300		300	
Total exposure (e <sup>-</sup> /Å <sup>2</sup> )	50		52	52	50		60	
Defocus range (μm)	-1.25 to -2.75		1.25 to -2.75	-1.25 to -2.75	-1.25 to -2.75		-1 to -2.25	
Calibrated physical pixel size (Å/px)	1.073		1.073	1.073	1.073		1.09	
<b>Reconstruction and refinement</b>								
Particles	446,530	118,725	334,903	407,623	421,738	236,327	264,418	
Map sharpening B factor	-116	-136	-98	-100	-121	-161	-10	
Resolution (Å)	3.6	4.5	3.8	3.6	3.4	3.9	3.2	
FSC Threshold	0.143	0.143	0.143	0.143	0.143	0.143	0.143	
<b>Model composition</b>								
RNA chains	1	-	1	1	1	1	-	
Protein chains	17	-	20	17	14	9	-	
<b>Model Building</b>								
Protein Geometry	Poor rotamers	0.00%	-	0.1%	0.00%	0.00%	0.12%	-
	Favored rotamers	95.47%	-	93.90%	96.08%	95.94%	96.71%	-
	Ramachandran outliers	0.21%	-	0.31%	0.00%	0.31%	0.00%	-
	Ramachandran favored	93.73%	-	92.28%	93.07%	91.60%	95.92%	-
	Cβ deviations >0.25Å	0.00%	-	0.00%	0.00%	0.00%	0.00%	-
	Bad bonds	0.00%	-	0.00%	0.00%	0.00%	0.00%	-
	Bad angles	0.00%	-	0.00%	0.00%	0.00%	0.00%	-
Nucleic Acid Geometry	Probably wrong sugar puckers	0.86%	-	1.12%	0.65%	0.58%	0.46%	-
	Bad backbone conformations	19.42%	-	27.38%	20.08%	16.76%	20.90%	-
	Bad bonds	0.00%	-	0.00%	0.00%	0.00%	0.00%	-
	Bad angles	0.03%	-	0.01%	0.00%	0.01%	0.00%	-
Low-resolution criteria	CaBLAM outliers	4.4%	-	4.4%	5.4%	6.0%	3.2%	-
	CA Geometry outliers	0.96%	-	0.94%	1.28%	1.00%	0.99%	-
Additional validations	Chiral Volumes outliers	0/9933	-	0/10342	0/9855	0/8827	0/5606	-